https://doi.org/10.5194/cp-2020-77
Preprint. Discussion started: 10 July 2020

Climate of the Past Discussions
Open Access
EGU

Atmospheric Fe supply has a negligible role in promoting marine productivity in the Glacial North Pacific Ocean

Francois Burgay[1,2], Andrea Spolaor [1,2*], Jacopo Gabrieli[1,2], Giulio Cozzi[1,2], Clara Turetta[1,2], Paul Vallelonga[3,4] and Carlo Barbante[1,2]

[1]Institute of Polar Sciences, National Research Council. Via Torino, 155, 3100 Venice (Italy)

[2]Department of Environmental Sciences, Informatics and Statistics, Ca' Foscari University of Venice. Via Torino, 155 – Venice (Italy)

[3]Physics of Ice Climate and Earth, Niels Bohr Institute, University of Copenhagen. Tagensvej 16, Copenhagen N2200 (Denmark)

[4]Oceans Graduate School, University of Western Australia (Australia)

* Corresponding author: andrea.spolaor@unive.it

Abstract

Iron is a key element in the Earth climate system as it can enhance the marine primary productivity in the High-Nutrient Low-Chlorophyll (HNLC) regions where, despite a high concentration of major nutrients, the chlorophyll production is low due to iron limitation. One of the main Fe sources to the ocean is aeolian dust. For this reason, ice cores provide a sensitive and continuous archive for reconstructing Fe fluxes over the last millennia. Here we show the first Northern Hemisphere Fe record retrieved from the NEEM ice core, which offers a unique opportunity to reconstruct the past Fe fluxes in the Arctic region over the last 108 kyr. Holocene Fe fluxes to the Arctic were three times lower than the average recorded over the last glacial period. They were greater during the Last Glacial Maximum (LGM) and the Marine Isotope Stage 4 (MIS 4). Comparing our data with palaeoceanographic records retrieved from the HNLC North Pacific, we demonstrated that during the coldest periods, characterized by the highest Fe fluxes, marine productivity in the subarctic Pacific Ocean did not increase due to a greater sea-ice extent and the absence of upwelling nutrient supply. This supports the hypothesis that Fe-fertilization was more effective in other regions, such as

https://doi.org/10.5194/cp-2020-77
Preprint. Discussion started: 10 July 2020

Climate of the Past Discussions

the transition zone of the North Pacific, where a closer relationship between marine productivity and the aeolian Fe fluxes was observed.

1. Introduction

Greenland and Antarctic ice cores are unique archives that can provide information about how temperature, atmospheric dust load and atmospheric gas composition have changed during the Holocene and the late Pleistocene (Lambert et al., 2008; Schüpbach et al., 2018). Glacial periods were dustier and with a lower CO_2 concentration (≈ 180 ppm) than interglacials (≈ 280 ppm). This dichotomy was explained through different hypotheses: the increase in aridity and in newly exposed continental shelves (Fuhrer et al., 1999), the enhancement of the atmospheric circulation (Delmas and Legrand, 1989), the increase in the aerosol atmospheric life-time (Yung et al., 1996), the enhancement of glacier mobilization of highly bioavailable iron from the bedrock (Shoenfelt et al., 2018) and, lastly, the enhancement of the polar circulation that might have entrained additional dust from lower latitudes (Mayewski et al., 1994). The higher atmospheric dust loading during glacial periods affected climate in both physical and biological ways. On the one hand, dust particles absorbed and scattered the incoming solar radiation and the outgoing infrared radiation with a direct effect on the Earth energy budget. On the other hand, once deposited on the ocean surface, the mineral dust provided major and micronutrients (including iron) that could have stimulated the biological carbon pump (Martin et al., 1990). This iron mediated mechanism has been demonstrated for the High-Nutrient Low-Chlorophyll (HNLC) regions, whose productivity is primarily Fe-limited, both through artificial (Smetacek et al., 2012; Yoon et al., 2018) and natural (Duprat et al., 2016; Langmann et al., 2010) Fe-fertilization processes. It has been inferred that the observed decrease in the atmospheric CO_2 concentration during glacial periods was linked to the Fe-modulated enhancement of the biological carbon pump in the Southern Ocean due to the increase in Fe availability (Martin et al., 1990). However, according to both modeling (Lambert et al., 2015) and observational (Gaspari et al., 2006; Röthlisberger, 2004; Vallelonga et al., 2013) studies, the Fe-fertilization mechanism itself cannot completely explain the ≈100 ppmv glacial-interglacial atmospheric CO_2 variability, but only around 8-20 ppmv of it.

Studies on leachable iron in ice cores were performed in Antarctica from Talos Dome (TD) (Spolaor et al., 2013; Vallelonga et al., 2013), Law Dome (LD) (Edwards et al., 2006; Edwards et al., 1998) and EPICA

https://doi.org/10.5194/cp-2020-77
Preprint. Discussion started: 10 July 2020


Climate of the Past Discussions

Dome C (DC) (Wolff et al., 2006). During the Holocene, the average flux and concentration values varied significantly among the different sites with similar values recorded at TD and LD and lower values at DC (Table 3). For TD, this was explained both through changes in atmospheric transport patterns across Antarctica and through a local input of dust from proximal Antarctic ice-free zones that affected coastal sites more than the central plateau (Albani et al., 2012; Delmonte et al., 2010; Vallelonga et al., 2013). During the LGM, the Fe fluxes were similar among the different Antarctic sites, suggesting a homogeneous atmospheric load over the entire Antarctic continent.

Unfortunately, few reconstructions of Arctic Fe fluxes exist and they are limited to the last centuries (Burgay et al., 2019; Hiscock et al., 2013). Reconstructing how the Fe concentrations and fluxes have changed in the Northern Hemisphere in the last millennia is essential to understand the evolution of the global atmospheric circulation, the human impact on dust mobilization (Mahowald et al., 2008) and to evaluate the impact on Marine Primary Production (MPP) in the North Pacific HNLC regions. Here, we present a 108 kyr record of leachable Fe retrieved from the North Greenland Eemian Ice Drilling (NEEM) ice core (Rasmussen et al., 2013; Schüpbach et al., 2018), which provides a unique insight on the iron supply in the Arctic both during the Holocene and the last Glacial. Furthermore, we performed a comparison between the Fe NEEM record and different palaeoproductivity records from the HNLC North Pacific region to evaluate if the increase in aeolian Fe fluxes was mirrored by an increase in marine productivity.

2. Materials and methods

2.1 Sampling site

In the framework of the NEEM project, a 2540 m-depth ice core was drilled in north-western Greenland (77°45'N, 51°06'W) at 2479 m.a.s.l. The site is characterized by an average annual temperature of -29°C and a modern accumulation of 22 cm ice equivalent per year. According to the GICC05modelext-NEEM-1 timescale, the ice core covers the last 128 kyrs (Rasmussen et al., 2013). The ice cores were cut to obtain ice sticks with a square cross section of 36x36 mm. They were continuously melted on a continuous flow analysis (CFA) system with a typical melt-speed of 3.5 cm min^{-1} (Schüpbach et al., 2018). A low-resolution (110 cm) sampling apparatus, collecting discrete samples for ICPMS analyses, was coupled to the CFA system. The CFA system provides meltwater from the inner and not contaminated part of the core, thus

https://doi.org/10.5194/cp-2020-77
Preprint. Discussion started: 10 July 2020


Climate of the Past Discussions
Open Access
EGU

we did not adopt any further decontamination procedure. The temporal resolution depends on the accumulation rate and it decreases with depth because of the ice thinning. According to the available timescale (Rasmussen et al., 2013) and considering the 110 cm sampling resolution, the temporal resolution varies from decadal to millennial (Table 1).

Samples were collected in vials previously cleaned as follows: 7 days with HNO_3 5% (Suprapure, Romil, UK), rinsed three times with Ultrapure water (UPW, Elga, UK), 7 days with HNO_3 2% % (Suprapure, Romil, UK), rinsed three times with UPW and dried under a laminar flow hood Class 100. The samples were kept frozen and shipped to Italy for analysis. Once melted, the samples were acidified to pH 1 using HNO_3 (Suprapure, Romil, UK). To ensure an effective dissolution of iron particles, samples were analysed 30 days after the acidification.

2.2 Analytical procedure and performances

The ice samples were analysed with an Inductively Coupled Plasma Single Quadrupole Mass Spectrometer (ICP-qMS, Agilent 7500 series, USA) equipped with a quartz Scott spray chamber. This allowed a comparison with previous studies on Antarctic ice cores (Gaspari et al., 2006; Vallelonga et al., 2013). To minimize any kind of contamination, all the instrument tubes were flushed before the analysis for 2 hours with 2% HNO_3 (Suprapure, Romil, UK). A 120 seconds rinsing step with 2% HNO_3 (Suprapure, Romil, UK) was performed after each sample to limit any possible memory effect, the vials used for the standard preparation were cleaned following the same procedure adopted for the ice samples. Considering the isobaric and polyatomic interferences affecting Fe, its quantification was performed using the interference-free isotope ^{57}Fe. Its quantification was performed using external calibration curves with acidified standards (2% HNO_3, Suprapure, Romil, UK) from dilution of a certified 1000 ppm ± 1% standard solution (Fisher Chemical, USA). The resulting R^2 for the external calibration curves was 0.999. The Limit of Detection (LoD) for ^{57}Fe, calculated as three times the standard deviation of the blank, was 0.8 µg L^{-1}. Accuracy and precision were evaluated using the TM-RAIN04 certified reference material produced by the National Research Council of Canada. The accuracy was determined as a recovery percentage calculated as O/T%, where O is the determined value and T is the certified value. For Fe, the accuracy was 104%, while precision, calculated as Relative Standard Deviation (RSD%), was 5%.

https://doi.org/10.5194/cp-2020-77
Preprint. Discussion started: 10 July 2020

Climate of the Past Discussions
Open Access
EGU

3. Results

3.1 Iron fluxes from the NEEM core

Iron concentrations and fluxes, calculated as F = C·A (where F is the Fe flux, expressed in mg m^{-2} yr^{-1}, C is the Fe concentration and A the accumulation, whose values are from Rasmussen et al., 2013) over the last 108 kyrs are reported in Table 2 and Figure 1. A pattern of higher dust (expressed as $nssCa^{2+}$) and Fe fluxes during colder climate periods and lower dust and Fe fluxes during warmer climate periods is clearly recognizable.

The Holocene (Figure 1) was characterized by average Fe fluxes of 0.06 mg m^{-2} yr^{-1} which varied between 0.01 mg m^{-2} yr^{-1} and 0.45 mg m^{-2} yr^{-1}. The Coefficient of Variability (CV), calculated as the ratio between the standard deviation and the mean value, was 1.2. The last 4000 years were characterized by the highest average Fe fluxes (0.09 ± 0.08 mg m^{-2} yr^{-1}). The lowest Fe fluxes were recorded between 4000 and 8000 years b2k (0.03 ± 0.02 mg m^{-2} yr^{-1}). During the Younger Dryas (YD, 11.7 – 12.9 kyr b2k), an abrupt cooling was observed with a drop in the $\delta^{18}O$ value from -36.9‰ to -43.1‰. The recorded average Fe fluxes were 0.13 ± 0.05 mg m^{-2} yr^{-1}, higher than both the 12.9-13.9 kyr b2k (0.06 ± 0.03 mg m^{-2} yr^{-1}) and the 10.7-11.7 kyr b2k (0.03 ± 0.02 mg m^{-2} yr^{-1}) periods.

The glacial period (11.7-108 kyr b2k) showed Fe fluxes three-times higher (0.2 mg m^{-2} yr^{-1}, CV = 1.0) than the Holocene, spanning from 0.01 to 1.80 mg m^{-2} yr^{-1} (Figure 1). A significant variability during the last glacial period was detected. During the LGM and MIS 4, average Fe fluxes were six (0.4 ± 0.3 mg m^{-2} yr^{-1}) and ten-times (0.6 ± 0.3 mg m^{-2} yr^{-1}) greater than the Holocene average. Fe fluxes also increased during MIS 5b (82-87 kyr b2k) when a concurrent decrease in $\delta^{18}O$ values was observed. During MIS 5c and MIS 5d, Fe fluxes were comparable with those detected during the Holocene. The high frequency of the Dansgaard-Oeschger (D-O) events that characterized MIS 3 is mirrored by the high variability in both nssCa and Fe fluxes. Each stadial period corresponded to an increase in both Fe and nssCa. However, their variability was significantly different. During MIS 3, Fe fluxes showed maxima values greater than 0.7 mg m^{-2} yr^{-1} during D-O 15, 13 and 5 (0.729, 0.819 and 0.933 mg m^{-2} yr^{-1} respectively), and lower than 0.3 mg m^{-2} yr^{-1} during D-O 12, 11, 10 and 8 (0.128, 0.274, 0.290 and 0.286 mg m^{-2} yr^{-1} respectively). This variability was significantly higher than the one recorded for nssCa, which showed maxima values closer to 2 mg m^{-2} yr^{-1} for

https://doi.org/10.5194/cp-2020-77
Preprint. Discussion started: 10 July 2020

all the D-O events. As an example, the nssCa maxima for D-O 15 and D-O 12 were 2.1 and 2.0 m^{-2} yr^{-1} respectively.

3.2 Comparison with Fe fluxes from Antarctic ice cores

The NEEM iron ice core record allows the first comparison of leachable Fe concentrations and fluxes between the Arctic and Antarctica (Figure 2) focusing on the Holocene, LGM and MIS 4 periods (Table 3).

During the Holocene, average Fe fluxes in both NEEM (0.06 mg m^{-2} yr^{-1}, CV = 1.2) and Talos Dome (0.09 mg m^{-2} yr^{-1}, CV = 1.2), were of the same order of magnitude suggesting a similar contribution from aeolian mineral dust in both sites. They were significantly greater than the ones recorded in Law Dome (0.04 mg m^{-2} yr^{-1}, CV = 0.5) and Dome C (0.007 mg m^{-2} yr^{-1}, CV = 0.2). As previously mentioned, the greater Fe fluxes in TD than in the other Antarctic sites, was related to the activation of a dust deflation area which influenced Victoria Land more than the central Antarctic Plateau (Delmonte et al., 2013).

The LGM (19 – 26.5 kyr b2k) showed Fe fluxes on the same order of magnitude among NEEM (0.4 mg m^{-2} yr^{-1}, CV = 0.6), TD (0.4 mg m^{-2} yr^{-1}, CV = 0.5), LD (0.4 mg m^{-2} yr^{-1}, CV = 0.7) and DC (0.2 mg m^{-2} yr^{-1}, CV = 0.5). Considering that the atmospheric CO_2 concentration dropped down to 180 ppm (Köhler et al., 2017), the global enhancement of the Fe fluxes likely contributed to part of this decrease, enhancing marine productivity in some HNLC regions (Amo and Minagawa, 2003; Kawahata et al., 2000; Martínez-Garcia et al., 2011)

MIS 4 (60-71 kyr b2k) was characterized by higher Fe fluxes in NEEM (0.6 mg m^{-2} yr^{-1}, CV = 0.5) than in Antarctica. Indeed, Fe fluxes both in TD (0.2 mg m^{-2} yr^{-1}, CV = 0.5) and DC (0.09 mg m^{-2} yr^{-1}, CV = 0.7) were substantially lower suggesting a particularly enhanced deflation from Asian deserts (e.g. high wind speeds, enhanced dustiness over the East Asian desert regions, increased aridity related to changes in the Asian monsoon system) (Schupbach et al., 2018).

3.3 Iron and marine productivity in the Northern Hemisphere

Considering the biological relevance of Fe and taking advantage from the Fe flux record retrieved from the NEEM ice core, we questioned if the increase in its fluxes triggered the marine productivity in the HNLC

https://doi.org/10.5194/cp-2020-77
Preprint. Discussion started: 10 July 2020


Climate of the Past Discussions
Open Access
EGU

region of the North Pacific. Our interpretation is based on Fe fluxes retrieved from samples, which were acidified with 2% HNO_3 for one month before the analysis. Therefore, they do not directly represent the actual bioavailable Fe that can be dissolved into seawater at pH 8, but rather an upper limit of the aeolian Fe potentially available for the phytoplankton (Edwards et al., 2006).

Geochemical evidence showed that the dust source that influences Greenland and the North Pacific is the same and it originates in both cases from the East Asian deserts (Schüpbach et al., 2018; Serno et al., 2014). A significant amount of Asian dust (250 Mt yr^{-1}) is mainly deposited over the HNLC region of the subarctic Pacific (Serno et al., 2014; Zhang et al., 2003) and the marine productivity changes in this oceanic region might reflect the possible Fe fertilization effects promoted by an increase in the atmospheric Fe supply. Both increases in aeolian influx from Asia (Young et al., 1991) and sporadic Fe input from volcanic eruptions (Langmann et al., 2010) caused an enhancement in MPP by more than 60% in this region. Moreover, Fe-fertilization experiments performed south of the Gulf of Alaska (McDonald et al., 1999; Tsuda et al., 2003), showed significant increases in the abundance of diatoms and in chlorophyll-a concentration (Boyd et al., 1996). This indicates that the North Pacific is rather sensitive to atmospheric iron inputs. However, no data are available to evaluate if the Fe-sensitivity of the subarctic Pacific Ocean holds over even longer timescales and if an increase in the aeolian Fe supply, observed during glacial periods, could explain the MPP variability in the subarctic Pacific Ocean. To address this point, we compared the NEEM Fe record with different marine sediment cores. For the period that ranges from the LGM to the Holocene we compared our record with the high-resolution SO202-27-6 (from the Patton-Murray Rise plateau, eastern subarctic Pacific Ocean) and the SO202-07-6 (from the Detroit Seamount, western subarctic Pacific Ocean) productivity records (Méheust et al., 2018). For a long-term record, we relied on the ODP887 (McDonald et al., 1999) and the ODP882 (Haug et al., 1995) sediment cores, located close to SO202-27-6 and SO202-07-6, respectively. A comparison over the last 108 kyr between the NEEM record and the S-2 sediment core (from the Shatsky Rise, transition zone) was also performed (Amo and Minagawa, 2003) (Figure 3, Table 4). This location shares, together with the northernmost sediment cores, the same Asian dust source and it is thus considered representative for the evaluation of the possible Fe-fertilization effects on MPP (Kawahata et al., 2000).

3.3.1 From the LGM to the Holocene

https://doi.org/10.5194/cp-2020-77
Preprint. Discussion started: 10 July 2020


Climate of the Past Discussions
Open Access
EGU

188 During the Last Glacial Maximum, the Fe fluxes recorded in the NEEM ice core were up to 7 times
189 higher than during the Holocene. However, marine productivity in the subarctic Pacific Ocean, expressed as
190 Si/Al ratio (McDonald et al., 1999), % biogenic silica (Haug et al., 1995) and Brassicasterol concentration
191 (Méheust et al., 2018), was at its lowest level (Figures 3, 4). Other records highlighted the same behaviour
192 with a minimum in palaeoproductivity during the LGM and a maximum during the Bølling-Allerød (B/A)
193 warm period (Ren et al., 2015). This can reflect the absence of key conditions that can intensify primary
194 production such as the presence of a well-developed water stratification (McDonald et al., 1999).

195 Reconstructions based on the foraminifera-bound $\delta^{15}N$ (FB-$\delta^{15}N$), a proxy which indicates the degree
196 of nitrate consumption by phytoplankton (Martínez-García et al., 2014), showed that, in the western
197 subarctic Pacific Ocean, the nitrate consumption was more complete during the LGM and the YD, when
198 MPP was low, than during the warmest periods (Ren et al., 2015). This apparent contradiction was explained
199 through an increase in the water stratification during the coldest periods (Francois et al., 1997) which led the
200 system towards a major-nutrient limitation. Indeed, the enhanced Fe supply from the aeolian mineral dust,
201 observed during the LGM and YD, determined an increase in the FB-$\delta^{15}N$ values, that is in the nitrate
202 consumption (Ren et al., 2015). However, because of the stronger water stratification (either by reduced
203 upwelling or vertical mixing), the nitrate supply from bottom waters was limited and this might have limited
204 the MPP (Kienast et al., 2004; Ren et al., 2015).

205 An additional explanation arises from the higher extent of perennial sea-ice that might have played a
206 role in creating a physical barrier between the atmosphere and the marine environment, reducing the amount
207 of available sunlight and the deposition of bioavailable Fe on seawater (Kienast et al., 2004; Méheust et al.,
208 2018). Marine sediment records, collected in the eastern and western subarctic Pacific and in the Bering Sea,
209 showed extended spring ice-cover during the LGM (Méheust et al., 2018; Méheust et al., 2016) when the Fe
210 fluxes were at their maxima. The progressive decrease in perennial sea-ice coverage recorded after the LGM
211 led to an increase in the marine productivity (Figure 4) with a maximum during the Bølling-Allerød (B/A)
212 warm event (≈ 13-15 kyr ago). The possible relevance of sea-ice in modulating MPP at the highest latitude of
213 the Pacific Ocean during the LGM is strengthened by a marine sediment record collected in the transition
214 zone (Amo and Minagawa, 2003), which, because of its southernmost location, did not experience any sea-
215 ice condition. During the LGM, contrarily to what is observed in the subarctic Pacific, a prominent

https://doi.org/10.5194/cp-2020-77
Preprint. Discussion started: 10 July 2020


Climate of the Past Discussions
Open Access
EGU

maximum in marine productivity was recorded, suggesting that Fe could have triggered an important phytoplankton response (Figure 4). The Fe-sensitivity of the transition zone is confirmed during the Holocene, when the Fe fluxes were at their minima and the productivity, expressed as MAR (Mass Accumulation Rate) C_{37} alkenone (μg cm^{-2} kyr^{-1}), was at its lowest level. A plausible explanation is that this region was not characterized by stratified waters and thus it was not affected by the limitation of major nutrients. Unfortunately, neither FB-$\delta^{15}N$ nor information about water stratification are available for this record.

3.3.1 From 108 kyr to the LGM

According to the available records, marine productivity changed heterogeneously in the Pacific Ocean during the last glacial period (Figure 3).

It is challenging to state, with a high degree of confidence, whether Fe-fertilization triggered a phytoplankton bloom or not in the HNLC subarctic North Pacific. This is due to the different responses that the western and the eastern sides showed with respect to the atmospheric iron supply (Figure 2). In the eastern subarctic Pacific, the increase in the Aeolian Fe fluxes was mirrored by a phytoplankton response during the MIS 5.2 and the MIS 5 / MIS 4 transition. The subsequent decrease in MPP during the MIS 4 suggests that the prolonged Fe supply during the coldest interstadial might have led the ecosystem towards the limitation of other nutrients (Kienast et al., 2014) following the similar mechanisms described in the previous section. The enhanced water stratification during those periods, as suggested by stable oxygen isotope ratios in planktonic foraminifera (Zahn et al., 1991), did not allow a supply of macronutrients from below the mixed layer. Thus, the additional atmospheric iron supply did not cause any additional effect on the phytoplankton, providing additional clues that their growth was likely limited by the lack of major nutrients (Kienast et al., 2004). In the western subarctic Pacific, the increase in productivity was recorded also in periods with low atmospheric Fe fluxes (e.g. from 100 to 90 kyr at ODP882), strengthening the hypothesis that other players (e.g. meltwater inputs, continental margin supply, sea-ice) had a more relevant role (Kienast et al., 2004; Lam and Bishop, 2008).

On the contrary to what was observed in the subarctic Pacific, the S-2 sediment core collected in the transition zone (Amo and Minagawa, 2003), showed a marked increase in primary productivity during MIS 4

https://doi.org/10.5194/cp-2020-77
Preprint. Discussion started: 10 July 2020

and the overall last glacial period when the Fe fluxes were higher (Figure 3). This indicates that the MPP in the transition zone of the North Pacific was sensitive to the atmospheric Fe supply, suggesting that the high degree of upper ocean stratification that characterized the subarctic region of the Pacific Ocean did not likely affect the transition zone. This, could have allowed a continuous supply of macronutrients so that the increase in dust transport (and Fe deposition) could have stimulated the productivity (Kienast et al., 2004).

4. Conclusions and future perspectives

In this study, we provided the first Fe record retrieved from the NEEM ice core. Through the comparison with other available Fe records, we observed that during the Holocene, the Fe fluxes were similar between TD and NEEM, while during the LGM all the investigated records showed Fe fluxes on the same order of magnitude. The greatest difference arose during the MIS 4, when Fe fluxes in NEEM were 3 and 7 times higher than in TD and DC respectively.

Merging our record with marine productivity data, we found that a direct link between Fe transport and ocean productivity holds only in the transition zone of the North Pacific. On the contrary, in the subarctic Pacific, we did not find any overwhelming evidence that the increase in the atmospheric Fe fluxes triggered a phytoplankton response. This indicates that other players, such as sea-ice and increased water stratification during the coldest periods have a more relevant role in modulating the MPP in the HNLC region of the North Pacific on a millennial time scale.

This study provided an upper limit for the potentially available Fe for the phytoplankton, meaning that other studies, that aim to analyse the most labile and bioavailable Fe fractions, are needed to better constrain the actual Fe bioavailability to the marine ecosystem.

Data availability

Data will be published on Pangaea

Author contributions

https://doi.org/10.5194/cp-2020-77
Preprint. Discussion started: 10 July 2020

FB wrote the manuscript. FB, AS and CB designed the research. JG, CT and GC performed the analyses. PV contributed to the interpretation of the results.

Competing interests

The authors declare that they have no conflict of interest.

Acknowledgments

We sincerely thank all the persons involved in the logistics, drilling operations, ice-core processing and sample collection. NEEM is directed and organized by the Center of Ice and Climate at the Niels Bohr Institute and US NSF Office of Polar Programs. It is supported by funding agencies and institutions in Belgium (FNRS-CFB and FWO), Canada (NRCan/GSC), China (CAS), Denmark (FIST), France (IPEV, CNRS/INSU, CEA and ANR), Germany (AWI), Iceland (RannIs), Japan (NIPR), Korea (KOPRI), The Netherlands (NWO/ALW), Sweden (VR), Switzerland (SNF), United Kingdom (NERC), and the USA (US NSF, Office of Polar Programs).

https://doi.org/10.5194/cp-2020-77
Preprint. Discussion started: 10 July 2020

Figures and tables

Figure 1 –$\delta^{18}O$ (blue line) profile is from the NGRIP ice core, while *nss*Ca^{2+} (red line) and Fe (black line) fluxes are from the NEEM ice core. YD: Younger Dryas, BA: Bølling-Allerød. Numbers in the bottom panel indicate the Dansgaard-Oeschger events.

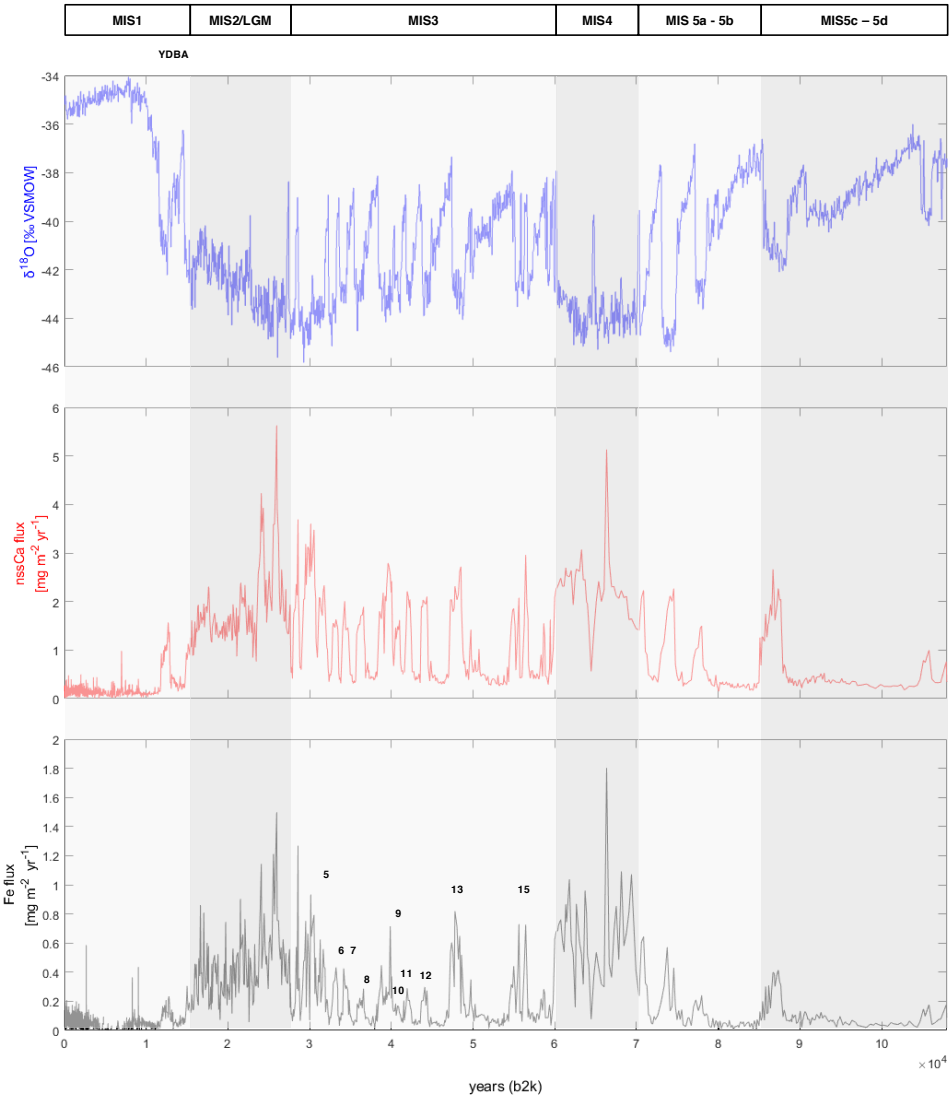

https://doi.org/10.5194/cp-2020-77
Preprint. Discussion started: 10 July 2020

Climate of the Past Discussions
Open Access
EGU

312

313 **Figure 2 –** Comparison of the Fe fluxes among NEEM (this work), TD (Vallelonga et al., 2013) and EDC
314 (Wolff et al., 2006)

315

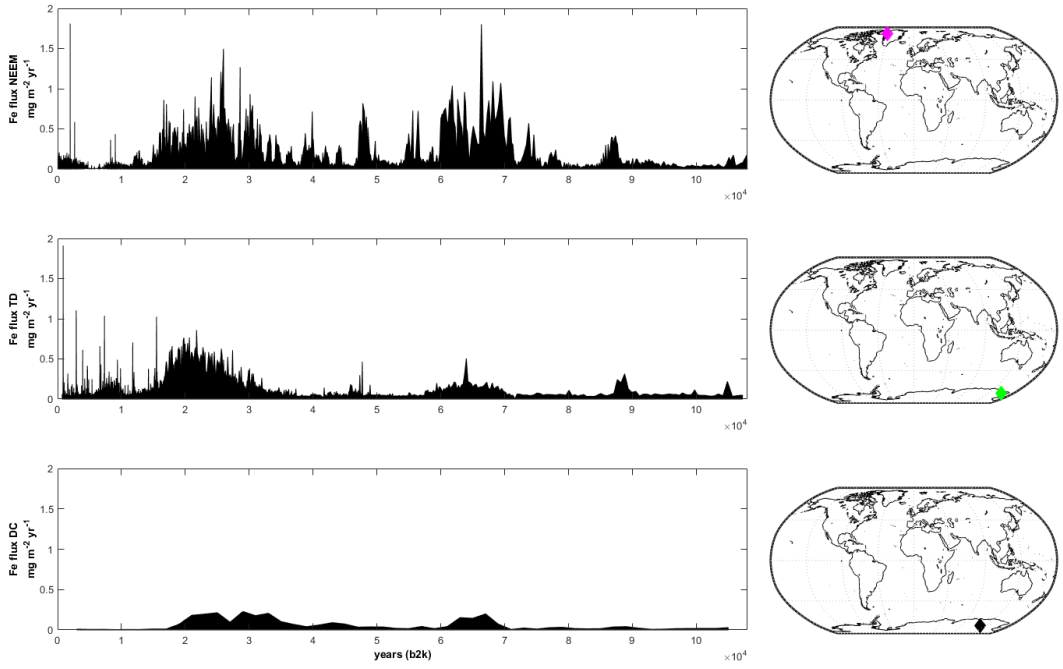

316

317

318

319

320

321

322

323

324

325

326

327

328

329

330

https://doi.org/10.5194/cp-2020-77
Preprint. Discussion started: 10 July 2020

Climate of the Past Discussions
Open Access
EGU

331

332 **Figure 3 –** Comparison between Fe fluxes (black line) from NEEM (this work), with marine productivity
333 (red lines) from ODP887, eastern subarctic Pacific (McDonald et al., 1999), ODP882, western subarctic
334 Pacific (Haug et al., 1995) and S-2, transition zone (Amo and Minagawa, 2003). Due to their limited
335 temporal extension, productivity records from SO202-07-6 and SO202-07-26 are not discussed in this figure,
336 but in Figure 4.

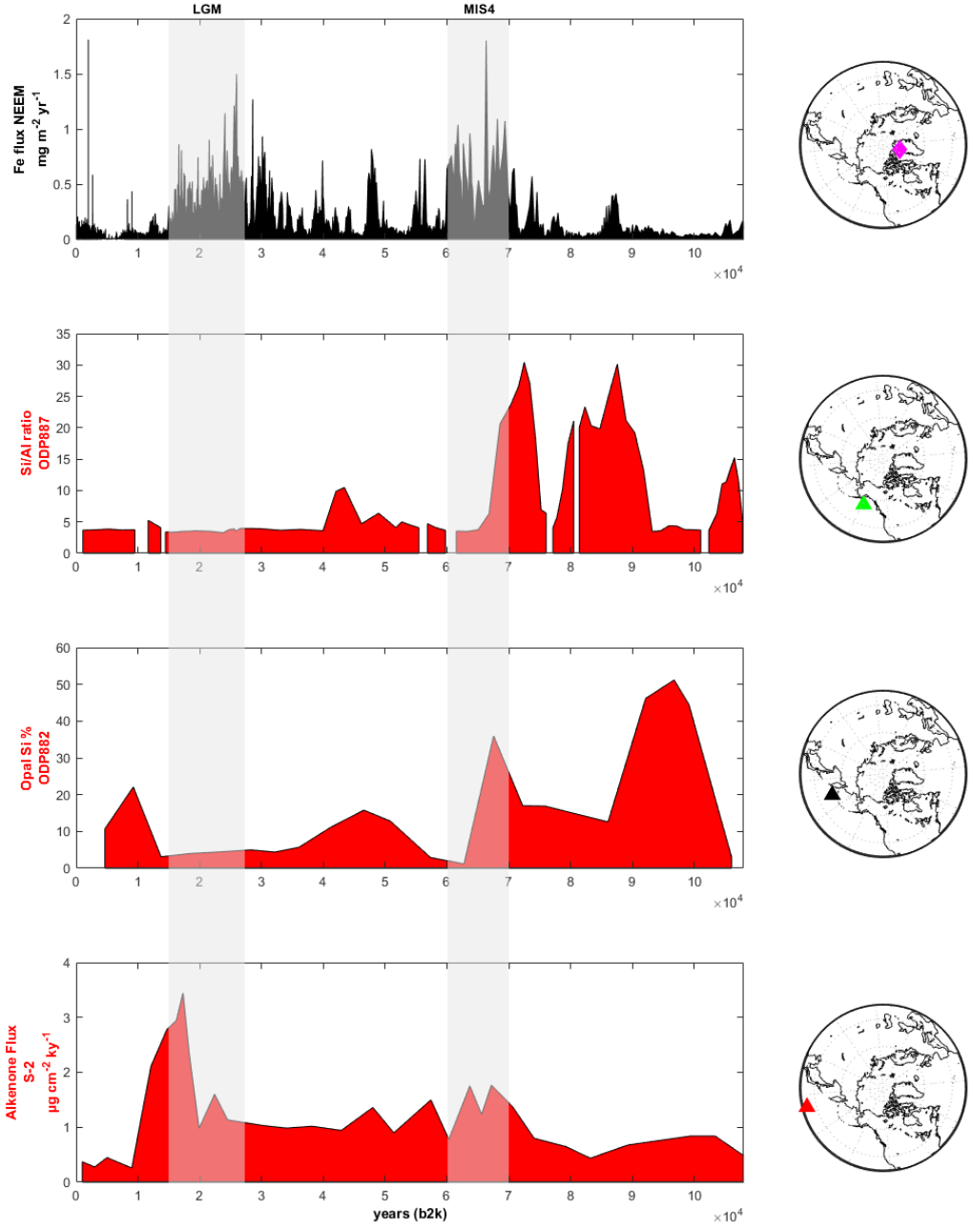

337

https://doi.org/10.5194/cp-2020-77
Preprint. Discussion started: 10 July 2020

Climate of the Past Discussions
Open Access
EGU

338 **Figure 4 –** Focus on the last 26 kyr and the possible influence of sea-ice in regulating MPP in the subarctic
339 Pacific Ocean. Sea-ice data are from Meheust et al. (2018): prevalently extended sea-ice (dark blue),
340 prevalently marginal sea-ice (blue), prevalently variable sea-ice (light blue), prevalently ice-free (white). Fe
341 flux record (black line), productivity in the eastern subarctic Pacific Ocean (SO202-07-6, red line, from
342 Meheust et al., (2018)), and productivity in the western subarctic Pacific Ocean (S0202-27-6, red line, from
343 Meheust et al (2018)). Productivity pulses were recorded when sea-ice changed its conditions towards ice-
344 free conditions. YD = Younger Dryas, B/A = Bolling-Allerod event, HS1 = Heinrich Stadial 1, LGM = Last
345 Glacial Maximum.

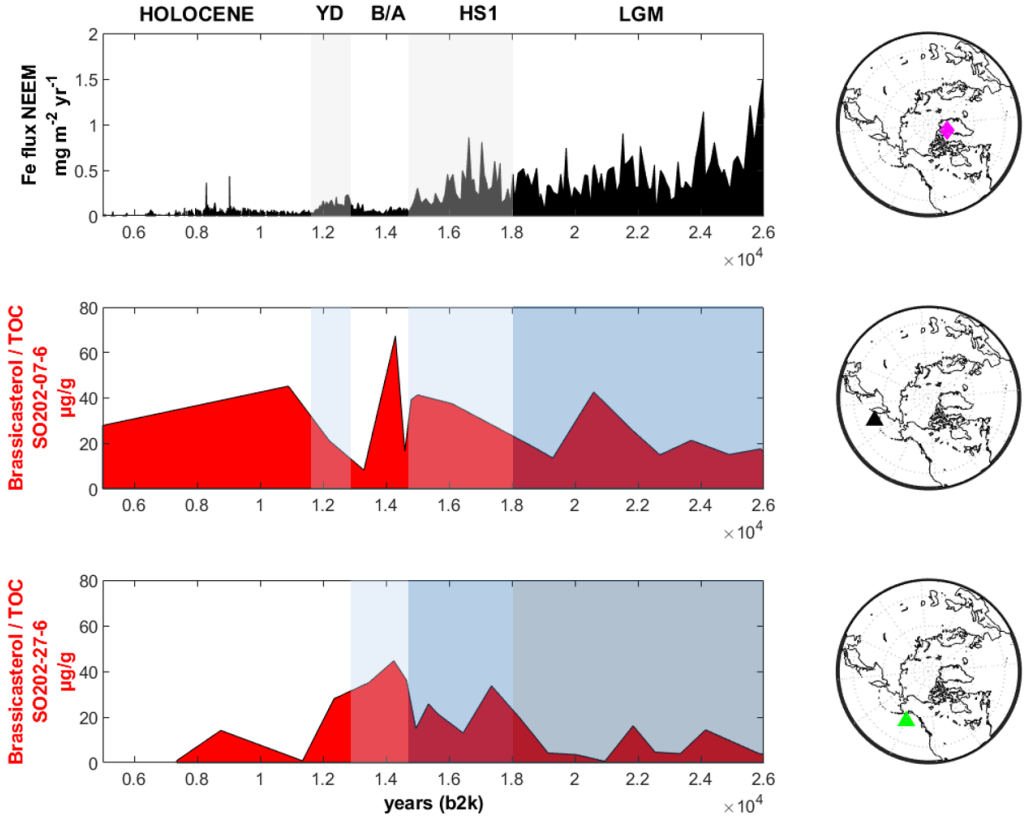

346

347

348

349

350

https://doi.org/10.5194/cp-2020-77
Preprint. Discussion started: 10 July 2020

Climate of the Past Discussions
Open Access
EGU

351 **Table 1 -** Ice samples for ICP-MS analysis were collected with a resolution of 110 cm. According to the
352 GICC05modelext-NEEM-1 age scale (Rasmussen et al., 2013), the temporal resolution is reported below.

353

Temporal resolution	Period
10 years	Holocene (post-7.2 kyr)
22 years	Holocene (pre-7.2 kyr)
110 years	Last Glacial Maximum
73 years	Interstadials
147 years	28-59 kyr
440 years	59-70 kyr
220 years	70-96 kyr
730 years	96-110 kyr

354

355

356

357 **Table 2 –** Fe average concentration (ng g^{-1}) and fluxes (mg m^{-2} yr^{-1}) from the NEEM ice core. More details in
358 the text. The Coefficient of Variability (CV) was calculated for Fe fluxes and it is reported in bold

	Fe average concentration /ng g^{-1}	Fe average fluxes /mg m^{-2} yr^{-1}
Holocene *(0.042 -11.7 kyr b2k)*	2.9	0.06 **(CV 1.2)**
Glacial *(11.7– 108 kyr b2k)*	44.3	0.2 **(CV 1.0)**
Younger Dryas *(11.7 – 12.9 kyr b2k)*	18.2	0.1 **(CV 0.4)**
LGM *(14.5 – 26.5 kyr b2k)*	86.3	0.4 **(CV 0.6)**
MIS 3 *(26.5 – 60 kyr b2k)*	45.5	0.2 **(CV 0.9)**
MIS 4 *(60 - 71 kyr b2k)*	146.4	0.6 **(CV 0.5)**
MIS 5a-MIS 5b *(71-87 kyr b2k)*	17.0	0.15 **(CV 1.0)**
MIS 5c-MIS 5d *(87-108 kyr b2k)*	6.5	0.07 **(CV 0.8)**

359

360

361

362

363

364

365

366

https://doi.org/10.5194/cp-2020-77
Preprint. Discussion started: 10 July 2020

Climate of the Past Discussions
Open Access
EGU

Table 3 – Comparison of Fe concentration ([Fe] in ng g^{-1}) and Fe fluxes (in mg m^{-2} yr^{-1}) among four different ice cores: NEEM, Talos Dome (Vallelonga et al., 2013), Law Dome (Edwards et al., 2006) and Dome C (Gaspari et al., 2006; Wolff et al., 2006). n.a. = not available. Fe concentration at DC is not available since the accumulation rate at that site during MIS4 is unavailable. Data from Law Dome spans from 59 to 8.5 b2k (for the Holocene) and from 18.2 to 23.7 b2k (for the LGM). The Coefficient of Variability (CV) was calculated for Fe fluxes and it is reported in bold for all the cores.

	Greenland		**Antarctica**					
	NEEM		**Talos Dome**		**Law Dome**		**Dome C**	
	[Fe] /ng g^{-1}	**Fe flux /mg m^{-2} yr^{-1}**	**[Fe] /ng g^{-1}**	**Fe flux /mg m^{-2} yr^{-1}**	**[Fe] /ng g^{-1}**	**Fe flux /mg m^{-2} yr^{-1}**	**[Fe] /ng g^{-1}**	**Fe flux /mg m^{-2} yr^{-1}**
Holocene *(0.042 - 11.7 kyr b2k)*	2.9	0.06 **(CV 1.2)**	1.4	0.09 **(CV 1.2)**	0.09	0.04 **(CV 0.5)**	0.2	0.007 **(CV 0.2)**
LGM *(14.5 -26.5 kyr b2k)*	86.3	0.4 **(CV 0.6)**	10.3	0.4 **(CV 0.5)**	2.4	0.4 **(CV 0.7)**	16	0.2 **(CV 0.5)**
MIS4 *(60- 71 kyr b2k)*	146.4	0.6 **(CV 0.5)**	3.1	0.2 **(CV 0.5)**	n.a.	n.a.	n.a.	0.09 **(CV 0.7)**

Table 4 – Summary of locations and data source for all the cores (both ice and sediment cores) discussed in the text (NH = Northern Hemisphere; SH = Southern Hemisphere)

Name	**Core**	**Location**	**Reference**	**Latitude/Longitude**
NEEM ice	Ice core	NH	*This work*	77°45'N, 51°06'W
Talos Dome	Ice core	SH	Vallelonga et al., 2013	73°0′S 158°0′E
Dome C	Ice core	SH	Wolff et al., 2006	75°06'S; 123°23' E
ODP882	Marine sediment	NH	Haug et al., 1995	50°22'N; 167°36'E
ODP887	Marine sediment	NH	McDonald et al., 1999	54°22'N; 148°27'W
SO202-27-6	Marine sediment	NH	Meheust et al., 2018	54°12'N; 149°36'W
SO202-07-6	Marine sediment	NH	Meheust et al., 2018	51°16'N; 167°42'E
SO202-18-6	Marine sediment	NH	Meheust et al., 2018	60°08'N; 179°26' W
S-2	Marine sediment	NH	Amo and Minagawa, 2003	33°22'N; 159°08'E

https://doi.org/10.5194/cp-2020-77
Preprint. Discussion started: 10 July 2020

Climate of the Past Discussions
Open Access
EGU

References

Albani, S., Delmonte, B., Maggi, V., Baroni, C., Petit, J. R., Stenni, B., Mazzola, C., and Frezzotti, M.: Interpreting last glacial to Holocene dust changes at Talos Dome (East Antarctica): implications for atmospheric variations from regional to hemispheric scales, Clim. Past, 8, 741-750, 2012.

Amo, M. and Minagawa, M.: Sedimentary record of marine and terrigenous organic matter delivery to the Shatsky Rise, western North Pacific, over the last 130 kyr, Organic Geochemistry, 34, 1299-1312, 2003.

Boyd, P., Muggli, D., Varela, D., Goldblatt, R., Chretien, R., Orians, K., and Harrison, P.: In vitro iron enrichment experiments in the NE subarctic Pacific, Marine Ecology Progress Series, 136, 179-193, 1996.

Burgay, F., Erhardt, T., Lunga, D. D., Jensen, C. M., Spolaor, A., Vallelonga, P., Fischer, H., and Barbante, C.: Fe2+ in ice cores as a new potential proxy to detect past volcanic eruptions, Science of The Total Environment, 654, 1110-1117, 2019.

Delmas, R. and Legrand, M.: Long-term changes in the concentrations of major chemical compounds (soluble and insoluble) along deep ice cores, The Environmental Record in Glaciers and Ice Sheets, 1989. 319-341, 1989.

Delmonte, B., Baroni, C., Andersson, P., Narcisi, B., Salvatore, M. C., Petit, J., Scarchilli, C., Frezzotti, M., Albani, S., and Maggi, V.: Modern and Holocene aeolian dust variability from Talos Dome (Northern Victoria Land) to the interior of the Antarctic ice sheet, Quaternary Science Reviews, 64, 76-89, 2013.

Delmonte, B., Baroni, C., Andersson, P. S., Schoberg, H., Hansson, M., Aciego, S., Petit, J.-R., Albani, S., Mazzola, C., Maggi, V., and Frezzotti, M.: Aeolian dust in the Talos Dome ice core (East Antarctica, Pacific/Ross Sea sector): Victoria Land versus remote sources over the last two climate cycles, Journal of Quaternary Science, 25, 1327-1337, 2010.

Duprat, L. P., Bigg, G. R., and Wilton, D. J.: Enhanced Southern Ocean marine productivity due to fertilization by giant icebergs, Nature Geoscience, 9, 219, 2016.

Edwards, R., Sedwick, P., Morgan, V., and Boutron, C.: Iron in ice cores from Law Dome: A record of atmospheric iron deposition for maritime East Antarctica during the Holocene and Last Glacial Maximum, Geochemistry, Geophysics, Geosystems, 7, 12, 2006.

Edwards, R., Sedwick, P. N., Morgan, V., Boutron, C. F., and Hong, S.: Iron in ice cores from Law Dome, East Antarctica: implications for past deposition of aerosol iron, Annals of Glaciology, 27, 365-370, 1998.

Francois, R., Altabet, M. A., Yu, E.-F., Sigman, D. M., Bacon, M. P., Frank, M., Bohrmann, G., Bareille, G., and Labeyrie, L. D.: Contribution of Southern Ocean surface-water stratification to low atmospheric CO 2 concentrations during the last glacial period, Nature, 389, 929-935, 1997.

Fuhrer, K., Wolff, E. W., and Johnsen, S. J.: Timescales for dust variability in the Greenland Ice Core Project (GRIP) ice core in the last 100,000 years, Journal of Geophysical Research: Atmospheres, 104, 31043-31052, 1999.

Gaspari, V., Barbante, C., Cozzi, G., Cescon, P., Boutron, C., Gabrielli, P., Capodaglio, G., Ferrari, C., Petit, J., and Delmonte, B.: Atmospheric iron fluxes over the last deglaciation: Climatic implications, Geophysical Research Letters, 33, 3, 2006.

https://doi.org/10.5194/cp-2020-77
Preprint. Discussion started: 10 July 2020

Haug, G., Maslin, M., Sarnthein, M., Stax, R., and Tiedemann, R.: 20. EVOLUTION OF NORTHWEST PACIFIC SEDIMENTATION PATTERNS SINCE 6 MA (SITE 882), 1995, 293.

Hiscock, W. T., Fischer, H., Bigler, M., Gfeller, G., Leuenberger, D., and Mini, O.: Continuous flow analysis of labile iron in ice-cores, Environmental science & technology, 47, 4416-4425, 2013.

Kawahata, H., Okamoto, T., Matsumoto, E., and Ujiie, H.: Fluctuations of eolian flux and ocean productivity in the mid-latitude North Pacific during the last 200 kyr, Quaternary Science Reviews, 19, 1279-1291, 2000.

Kienast, S. S., Hendy, I. L., Crusius, J., Pedersen, T. F., and Calvert, S. E.: Export production in the subarctic North Pacific over the last 800 kyrs: No evidence for iron fertilization?, Journal of Oceanography, 60, 189-203, 2004.

Köhler, P., Nehrbass-Ahles, C., Schmitt, J., Stocker, T. F., and Fischer, H.: Continuous record of the atmospheric greenhouse gas carbon dioxide (CO2), raw data. In: In supplement to: Köhler, P et al. (2017): A 156 kyr smoothed history of the atmospheric greenhouse gases CO2, CH4, and N2O and their radiative forcing. Earth System Science Data, 9(1), 363-387, https://doi.org/10.5194/essd-9-363-2017, PANGAEA, 2017.

Lam, P. and Bishop, J. K. B.: The continental margin is a key source of iron to the HNLC North Pacific Ocean, Geophysical Research Letters, 35, 7, 2008.

Lambert, F., Delmonte, B., Petit, J.-R., Bigler, M., Kaufmann, P. R., Hutterli, M. A., Stocker, T. F., Ruth, U., Steffensen, J. P., and Maggi, V.: Dust-climate couplings over the past 800,000 years from the EPICA Dome C ice core, Nature, 452, 616, 2008.

Lambert, F., Tagliabue, A., Shaffer, G., Lamy, F., Winckler, G., Farias, L., Gallardo, L., and De Pol-Holz, R.: Dust fluxes and iron fertilization in Holocene and Last Glacial Maximum climates, Geophysical Research Letters, 42, 6014-6023, 2015.

Langmann, B., Zakšek, K., Hort, M., and Duggen, S.: Volcanic ash as fertiliser for the surface ocean, Atmospheric Chemistry and Physics, 10, 3891-3899, 2010.

Mahowald, N. M., Engelstaedter, S., Luo, C., Sealy, A., Artaxo, P., Benitez-Nelson, C., Bonnet, S., Chen, Y., Chuang, P. Y., Cohen, D. D., Dulac, F., Herut, B., Johansen, A. M., Kubilay, N., Losno, R., Maenhaut, W., Paytan, A., Prospero, J. M., Shank, L. M., and Siefert, R. L.: Atmospheric Iron Deposition: Global Distribution, Variability, and Human Perturbations, Annual Review of Marine Science, 1, 245-278, 2008.

Martin, J. H., Gordon, R. M., and Fitzwater, S. E.: Iron in Antarctic waters, Nature, 345, 156-158, 1990.
Martínez-Garcia, A., Rosell-Melé, A., Jaccard, S. L., Geibert, W., Sigman, D. M., and Haug, G. H.: Southern Ocean dust–climate coupling over the past four million years, Nature, 476, 312, 2011.

Martínez-García, A., Sigman, D. M., Ren, H., Anderson, R. F., Straub, M., Hodell, D. A., Jaccard, S. L., Eglinton, T. I., and Haug, G. H.: Iron fertilization of the Subantarctic Ocean during the last ice age, Science, 343, 1347-1350, 2014.

Mayewski, P. A., Meeker, L. D., Whitlow, S., Twickler, M. S., Morrison, M. C., Bloomfield, P., Bond, G., Alley, R. B., Gow, A. J., and Meese, D. A.: Changes in atmospheric circulation and ocean ice cover over the North Atlantic during the last 41,000 years, Science, 263, 1747-1751, 1994.

McDonald, D., Pedersen, T., and Crusius, J.: Multiple late Quaternary episodes of exceptional diatom production in the Gulf of Alaska, Deep Sea Research Part II: Topical Studies in Oceanography, 46, 2993-3017, 1999.

https://doi.org/10.5194/cp-2020-77
Preprint. Discussion started: 10 July 2020

Méheust, M., Stein, R., Fahl, K., and Gersonde, R.: Sea-ice variability in the subarctic North Pacific and adjacent Bering Sea during the past 25 ka: new insights from IP 25 and U k' 37 proxy records, arktos, 4, 8, 2018.

Méheust, M., Stein, R., Fahl, K., Max, L., and Riethdorf, J.-R.: High-resolution IP 25-based reconstruction of sea-ice variability in the western North Pacific and Bering Sea during the past 18,000 years, Geo-Marine Letters, 36, 101-111, 2016.

Rasmussen, S. O., Abbott, P. M., Blunier, T., Bourne, A. J., Brook, E., Buchardt, S. L., Buizert, C., Chappellaz, J., Clausen, H. B., Cook, E., Dahl-Jensen, D., Davies, S. M., Guillevic, M., Kipfstuhl, S., Laepple, T., Seierstad, I. K., Severinghaus, J. P., Steffensen, J. P., Stowasser, C., Svensson, A., Vallelonga, P., Vinther, B. M., Wilhelms, F., and Winstrup, M.: A first chronology for the North Greenland Eemian Ice Drilling (NEEM) ice core, Clim. Past, 9, 2713-2730, 2013.

Ren, H., Studer, A. S., Serno, S., Sigman, D. M., Winckler, G., Anderson, R. F., Oleynik, S., Gersonde, R., and Haug, G. H.: Glacial-to-interglacial changes in nitrate supply and consumption in the subarctic North Pacific from microfossil-bound N isotopes at two trophic levels, Paleoceanography, 30, 1217-1232, 2015.

Röthlisberger, R.: Ice core evidence for the extent of past atmospheric CO2change due to iron fertilisation, Geophysical Research Letters, 31, 16, 2004.

Schüpbach, S., Fischer, H., Bigler, M., Erhardt, T., Gfeller, G., Leuenberger, D., Mini, O., Mulvaney, R., Abram, N. J., and Fleet, L.: Greenland records of aerosol source and atmospheric lifetime changes from the Eemian to the Holocene, Nature communications, 9, 1476, 2018.

Serno, S., Winckler, G., Anderson, R. F., Hayes, C. T., McGee, D., Machalett, B., Ren, H., Straub, S. M., Gersonde, R., and Haug, G. H.: Eolian dust input to the Subarctic North Pacific, Earth and Planetary Science Letters, 387, 252-263, 2014.

Shoenfelt, E. M., Winckler, G., Lamy, F., Anderson, R. F., and Bostick, B. C.: Highly bioavailable dust-borne iron delivered to the Southern Ocean during glacial periods, Proceedings of the National Academy of Sciences, 115, 11180-11185, 2018.

Smetacek, V., Klaas, C., Strass, V. H., Assmy, P., Montresor, M., Cisewski, B., Savoye, N., Webb, A., d'Ovidio, F., and Arrieta, J. M.: Deep carbon export from a Southern Ocean iron-fertilized diatom bloom, Nature, 487, 313-319, 2012.

Spolaor, A., Vallelonga, P., Cozzi, G., Gabrieli, J., Varin, C., Kehrwald, N., Zennaro, P., Boutron, C., and Barbante, C.: Iron speciation in aerosol dust influences iron bioavailability over glacial-interglacial timescales, Geophysical Research Letters, 40, 1618-1623, 2013.

Tsuda, A., Takeda, S., Saito, H., Nishioka, J., Nojiri, Y., Kudo, I., Kiyosawa, H., Shiomoto, A., Imai, K., and Ono, T.: A mesoscale iron enrichment in the western subarctic Pacific induces a large centric diatom bloom, Science, 300, 958-961, 2003.

Vallelonga, P., Barbante, C., Cozzi, G., Gabrieli, J., Schüpbach, S., Spolaor, A., and Turetta, C.: Iron fluxes to Talos Dome, Antarctica, over the past 200 kyr, Clim. Past, 9, 597-604, 2013.

Wolff, E. W., Fischer, H., Fundel, F., Ruth, U., Twarloh, B., Littot, G. C., Mulvaney, R., Röthlisberger, R., De Angelis, M., and Boutron, C. F.: Southern Ocean sea-ice extent, productivity and iron flux over the past eight glacial cycles, Nature, 440, 491-496, 2006.

https://doi.org/10.5194/cp-2020-77
Preprint. Discussion started: 10 July 2020

536 Yoon, J.-E., Yoo, K.-C., Macdonald, A. M., Yoon, H.-I., Park, K.-T., Yang, E. J., Kim, H.-C., Lee, J. I., Lee, M. K.,
537 and Jung, J.: Reviews and syntheses: Ocean iron fertilization experiments–past, present, and future looking
538 to a future Korean Iron Fertilization Experiment in the Southern Ocean (KIFES) project, Biogeosciences, 15,
539 5847-5889, 2018.
540
541 Young, R., Carder, K., Betzer, P., Costello, D., Duce, R., DiTullio, G., Tindale, N., Laws, E., Uematsu, M., and
542 Merrill, J.: Atmospheric iron inputs and primary productivity: Phytoplankton responses in the North Pacific,
543 Global Biogeochemical Cycles, 5, 119-134, 1991.
544
545 Yung, Y. L., Lee, T., Wang, C.-H., and Shieh, Y.-T.: Dust: A diagnostic of the hydrologic cycle during the Last
546 Glacial Maximum, Science, 271, 962-963, 1996.
547
548 Zahn, R., Pedersen, T. F., Bornhold, B. D., and Mix, A. C.: Water mass conversion in the glacial subarctic
549 Pacific (54° N, 148° W): Physical constraints and the benthic-planktonic stable isotope record,
550 Paleoceanography, 6, 543-560, 1991.
551
552 Zhang, X.-Y., Gong, S., Zhao, T., Arimoto, R., Wang, Y., and Zhou, Z.: Sources of Asian dust and role of
553 climate change versus desertification in Asian dust emission, Geophysical Research Letters, 30, 2003.
554